Bonding Analysis in Inorganic Transition-Metal Cubic Clusters. 2. Metal-Centered Hexacapped $M_9(\mu_4\text{-}E)_6L_8$ Species

Eric Furet, Albert Le Beuze, Jean-François Halet,* and Jean-Yves Saillard*

Contribution from the Laboratoire de Chimie du Solide et Inorganique Moléculaire, URA CNRS 1495, Université de Rennes I, 35042 Rennes Cedex, France

Received March 28, 1994[⊗]

Abstract: The bonding in metal-centered $M_9(\mu_4\text{-}E)_6L_8$ cubic clusters is analyzed by means of extended Hückel and self-consistent field−multiple scattering−Xα calculations. Different electron counts are allowed depending on the magnitude of the interaction of the interstitial metal atom (M_c) with its metallic cubic host (M_s) *and* the nature of the capping E ligands (either bare or substituted). In all cases, a strong interaction is observed between the s and p AOs of the encapsulated atom and metallic MOs of the cube. Significant additional M_c-M_s bonding is obtained if strong interactions occur between the five d AOs and corresponding metallic MOs. This still hypothetical situation, which leads to a count of 120 metallic valence electrons (MVEs), is favored for long M_s-M_s and short M_c-E contacts. Another closed-shell configuration, corresponding to 124 MVEs, is obtained if the interaction of the M_c t_{2g} d AOs with the metallic cube is large and the e_g one weak. This is the case for $Ni_9(\mu_4\text{-}GeEt)_6(CO)_8$. Electron counts corresponding to open-shell ground-state configurations can occur when the capping E ligands are strong donors and/or when the MVE count is larger than 120. In such cases, the levels which may be partly populated are of e_g, t_{2g}, and (for large electron counts) t_{1g} symmetry. For example, the ground-state electron distribution of the 124-MVE clusters $Pd_9(\mu_4\text{-}E)_6(PPh_3)_8$ (E = As, Sb) corresponds to $(t_{2g})^4(e_g)^0(t_{1g})^0$, while it is found to be $(e_g)^4(t_{1g})^4(t_{2g})^2$ for the 130-MVE cluster $Ni_9(\mu_4\text{-}Te)_6(PEt_3)_8$. The various possibilities for the electron distribution in these levels are discussed for various MVE counts, in relation to the M−M and M−E bond distances and the nature of E. The possibility of incorporating main-group elements at the center of the metallic cube is also discussed.

Introduction

In a previous paper we have analyzed the electronic structure of various metallic cubic clusters of the type $M_8(\mu_4\text{-}E)_6L_8$, where M is a transition-metal, E a main-group atom or a conical fragment such as S, Se, PR, or GeR, and L a 2-electron ligand like CO, PR_3, Cl^-, ...[1] We have shown that the optimal number of metallic valence electrons (MVEs) for these species is 120, which is favored with electronegative metals and/or π-acceptor terminal ligands. A rather strong M−M bonding is present in these species, mainly due to through-space M−M interactions but also via through-bond M−E interactions. For such an electron count, the M−(μ_4-E) bonding is maximized, whereas the M−M bonding is not. The latter is strengthened upon depopulation of the top of the d band, which is weakly antibonding. Electron counts lower than 120 MVEs and open-shell configurations are then possible for clusters bearing terminal π-donor ligands. The possible depopulation of the top of the metallic d band allows a large range of electron counts (from 120 to 99 so far) without altering the cubic metallic core. The count of 76 MVEs constitutes the lowest hypothetical limit for these cubic species, which preserves the M−M cubane-type bonding mode.

Efforts to incorporate elements into the metallic cube of these clusters have given rise to a new class of electron-rich compounds of formula $M_9(\mu_4\text{-}E)_6L_8$, where a metal atom is "swallowed" in the middle of the metallic cubic core, as exemplified by $Ni_9(\mu_4\text{-}GeEt)_6(CO)_8$ (**1**, Chart 1).[2] Several metal-centered hexacapped cubic $M_9(\mu_4\text{-}E)_6L_8$ clusters analogous to

Chart 1

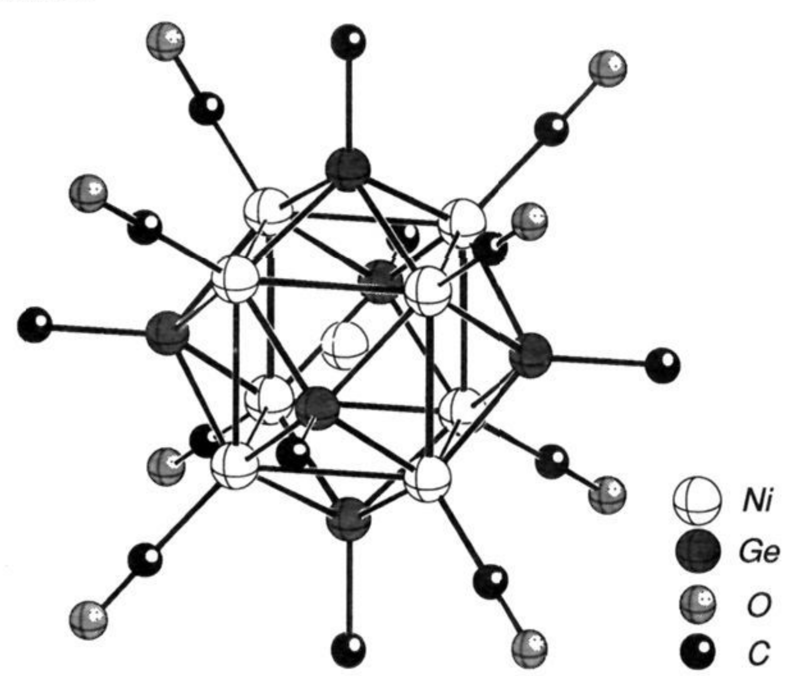

1 have been structurally characterized. They are listed in Table 1 along with some relevant data. These compounds, known only for M = Ni or Pd so far, exhibit MVE counts varying from 121 to 130, whereas their noncentered $M_8(\mu_4\text{-}E)_6L_8$ parents possess a maximum of 120 MVEs.[1] Application of the 18-electron rule to these M_9 species leads to a count of $(18 \times 9) - (20 \times 2) = 122$ MVEs, assuming 20 two-center/two-electron bonds (12 M_s-M_s and 8 M_c-M_s, where M_s and M_c are surface metal and central metal, respectively). Only one example (compound **3** in Table 1) bears this electron count.[4] In fact,

[⊗] Abstract published in *Advance ACS Abstracts*, April 15, 1995.

(1) Part 1: Furet, E.; Le Beuze, A.; Halet, J.-F.; Saillard, J.-Y. *J. Am. Chem. Soc.* **1994**, *116*, 274. See also: Rösch, N.; Ackermann, L.; Pacchioni, G. *Inorg. Chem.* **1993**, *32*, 2963.
(2) Zebrowski, J. P.; Hayashi, R. K.; Bjarnason, A.; Dahl, L. F. *J. Am. Chem. Soc.* **1992**, *114*, 3121.
(3) Fenske, D.; Persau, C. *Z. Anorg. Allg. Chem.* **1991**, *593*, 61.
(4) Fenske, D.; Ohmer, J.; Merzweiler, K. *Angew. Chem., Int. Ed. Engl.* **1988**, *27*, 1512.
(5) Brennan, J. G.; Siegrist, T.; Stuczynski, S. M.; Steigerwald, M. L. *J. Am. Chem. Soc.* **1989**, *111*, 9240.
(6) Fenske, D.; Fleischer, H.; Persau, C. *Angew. Chem., Int. Ed. Engl.* **1989**, *28*, 1665.

0002-7863/95/1517-4936$09.00/0

Table 1. Metal-Centered Molecular Cubic $M_9(\mu_4\text{-}E)_6L_8$ Clusters Characterized by X-ray Diffraction

compd	$d(M_s-M_s)^a$	$d(M_c-E)/(d(M_s-E)^b$	MVE^c	color	ref
$Ni_9(\mu_4\text{-}GeEt)_6(CO)_8$ (**1**)	2.67	1.17	124	red	2
$Ni_9(\mu_4\text{-}P)_6(PCy_3)_6Cl_2$ (**2**)	2.80	1.10	122		3
$Ni_9(\mu_4\text{-}As)_6(PPh_3)_6Cl_2$ (**3**)	2.81	1.13	122	black	4
$Ni_9(\mu_4\text{-}As)_6(PPh_3)_5Cl_3$ (**4**)	2.81	1.13	121	black	4
$Ni_9(\mu_4\text{-}Te)_6(PEt_3)_8$ (**5**)	2.86	1.17	130		5
$Pd_9(\mu_4\text{-}As)_6(PPh_3)_8$ (**6**)	3.11	1.09	124	black	6
$Pd_9(\mu_4\text{-}Sb)_6(PPh_3)_8$ (**7**)	3.26	1.10	124	black	3

^{a} Averaged surface metal−surface metal distance (Å). ^{b} Ratio between interstitial metal-capping atom and surface metal-capping atom distances. ^{c} Total valence metallic electron count.

group theory indicates that a set of eight localized M_c-M_s σ-bonds form a reducible representation, which decomposes in ($a_{1g} + a_{2u} + t_{2g} + t_{1u}$) under O_h symmetry. This means that the central metal atom must possess among its nine valence atomic orbitals (AOs) a set of eight which corresponds to these irreducible representations. This requirement is not completely satisfied since there is no a_{2u} AO on the central metal atom. Consequently, the localized two-center/two-electron bonding scheme on which the 18-electron rule is based cannot apply. A delocalized approach is then necessary to describe the metallic bonding mode in the $M_9(\mu_4\text{-}E)_6L_8$ compounds. This is reminiscent of that observed in metallic body-centered-cubic extended structures.

Such a delocalized picture is provided for cluster compounds by the well-known Polyhedral Skeletal Electron Pair Theory.[7] Within this framework, Mingos and collaborators have shown that the electron count for high nuclearity compounds with an interstitial metal atom is usually governed by the $12N_s + \Delta_i$ rule, where N_s is the number of surface metal atoms (M_s) and Δ_i a characteristic electron number, which depends on the importance of radial and tangential metal−metal bonding (usually 18 or 24).[7] According to this electron-counting procedure, known as the *inclusion principle*,[7] the M_9 compounds given in Table 1 should possess either 114 or 120 MVEs. The actual electron counts observed for the cubic clusters containing an encapsulated transition-metal atom show that these electron-counting rules do not apply properly for this class of compounds (see Table 1).

Few theoretical works have been devoted to this family of compounds. From extended Hückel (EH) calculations on a simplified model of the 130-MVE compound **5**, Wheeler also suggested the possibility of favored MVE counts of 120 and 126.[8] More recently, Nomikou and collaborators have used EH calculations to re-examine the electronic structure of the molecular cubic cluster $Ni_9(\mu_4\text{-}Te)_6(PH_3)_8$ in order to draw relationships with nickel−tellurium extended structures.[9] To date, however, no complete rationalization has been done on the whole set of clusters listed in Table 1. This paper utilizes extended Hückel (EH) and self-consistent field−multiple scattering−Xα (Xα) calculations to understand the bonding in these clusters, as a function of different parameters, such as the electron count or the nature and the size of the different elements constituting the cluster cage. We shall particularly focus on the role of the interstitial metal atom on the electronic structure of the cubic clusters. The computational details are given in the Appendix.

Qualitative Approach

The electronic structure of the $M_9(\mu_4\text{-}E)_6L_8$ compounds can be described as resulting from the interaction between the interstitial metal atom and its $M_8(\mu_4\text{-}E)_6L_8$ host. The existence of M_c-M_s bonding implies that there is also some M_s-M_s bonding. Indeed, for a regular cube, the latter contact is only 1.15 times longer than the former. From our previous study on noncentered cubic species, one can deduce that the existence of M_s-M_s bonding on the $M_8(\mu_4\text{-}E)_6L_8$ cage leads to a significant energy gap between the nonbonding or weakly antibonding d-block and the levels which are really antibonding. This is the energy gap which secures the favored count of 120 MVEs in the real $M_8(\mu_4\text{-}E)_6L_8$ compounds.[1] Among the 60 occupied levels, 34 constitute the d-block with the following electron distribution $(1 \times a_{1g})^2(2 \times e_g)^8(1 \times t_{1g})^6(3 \times t_{2g})^{18}(1 \times a_{2u})^2(2 \times e_u)^8(2 \times t_{1u})^{12}(2 \times t_{2u})^{12}$.[1] For the sake of simplicity, the electron configuration of stable 120-MVE $M_8(\mu_4\text{-}E)_6L_8$ species will be written in the following discussion as [120]. This general situation for the $M_8(\mu_4\text{-}E)_6L_8$ cage is given schematically in the middle of Figure 1.

The nine AOs of the interstitical metal atom span a_{1g} (s) + t_{1u} (x, y, z) + e_g ($x^2 - y^2, z^2$) + t_{2g} (xy, xz, yz). Strong bonding interactions are expected between its high-lying diffuse s (a_{1g}) and p (t_{1u}) AOs and some corresponding levels of the d-block of the metallic cage. As a consequence, the high-lying s and p AOs of M_c are strongly destabilized and cannot be populated (see Figure 1). This is a common situation in transition-metal compounds and means that when the M_c atom is introduced in the middle of the cage, the a_{1g} and t_{1u} interactions do not change the number of low-lying levels, and therefore are not expected to change the favored 120-MVE count of the $M_8(\mu_4\text{-}E)_6L_8$ cage.

Such a result is not so straightforward for the interactions involving the low-lying and more contracted d AOs of M_c, which decompose into e_g ($x^2 - y^2, z^2$) and t_{2g} (xy, xz, yz) under O_h symmetry. Indeed, four different closed-shell cases leading to four different MVE counts can be predicted *a priori*, depending on the strength of the interaction of the M_c d orbitals with corresponding M_8 levels. (1) If both e_g and t_{2g} AOs of M_c interact strongly with some corresponding metallic levels of the cage, the resulting out-of-phase combinations will be sufficiently antibonding to lie at high energy and will not be occupied. The electron count of 120 then remains unchanged (electron configuration [120], see Figure 1a) and strong M_c-M_s bonding is expected. (2) If both the e_g and t_{2g} orbitals interact weakly, the out-of-phase combinations will remain at a relatively low energy and therefore will be occupied (see Figure 1b). This increases by five the number of levels in the cluster d-block. Therefore, the favored MVE count is 120 + 10 = 130, corresponding to the $[120](e_g)^4(t_{2g})^6$ configuration. The M_c-M_s bonding is only ensured by the interaction of the M_c s and p AOs with some cage counterparts. (3) When only the t_{2g} interaction is strong, while the e_g interaction is weak, the favored electron count will be 120 + 4 = 124 (configuration $[120](e_g)^4$, see Figure 1c). (4) When the e_g interaction is strong and the t_{2g} interaction is weak, the favored electron count will be 120 + 6 = 126 (configuration $[120](t_{2g})^6$, see Figure 1d). In the following sections we analyze the compounds listed in Table 1 to see whether or not they satisfy the closed-shell electron configurations shown in Figure 1.

The 124-Electron Cluster Model $Ni_9(\mu_4\text{-}GeH)_6(CO)_8$

The EH and Xα molecular orbital (MO) diagrams of the 124-electron cluster $Ni_9(\mu_4\text{-}GeH)_6(CO)_8$, used to model compound

(7) (a) See for example: Mingos, D. M. P.; Wales, D. J. *Introduction to Cluster Chemistry*; Prentice-Hall International Editions: Englewood Cliffs, 1990. (b) Mingos, D. M. P. *J. Chem. Soc., Chem. Commun.* **1985**, 1353. (c) Mingos, D. M. P.; Johnston, R. L. *Struct. Bond. (Berlin)* **1987**, *68*, 29. (d) Mingos, D. M. P.; Lin, Z. *J. Chem. Soc., Dalton Trans.* **1988**, 1657 and references therein.

(8) Wheeler, R. A. *J. Am. Chem. Soc.* **1990**, *112*, 8737; **1991**, *113*, 4046.

(9) Nomikou, Z.; Schubert, B.; Hoffmann, R.; Steigerwald, M. L. *Inorg. Chem.* **1992**, *31*, 2201.

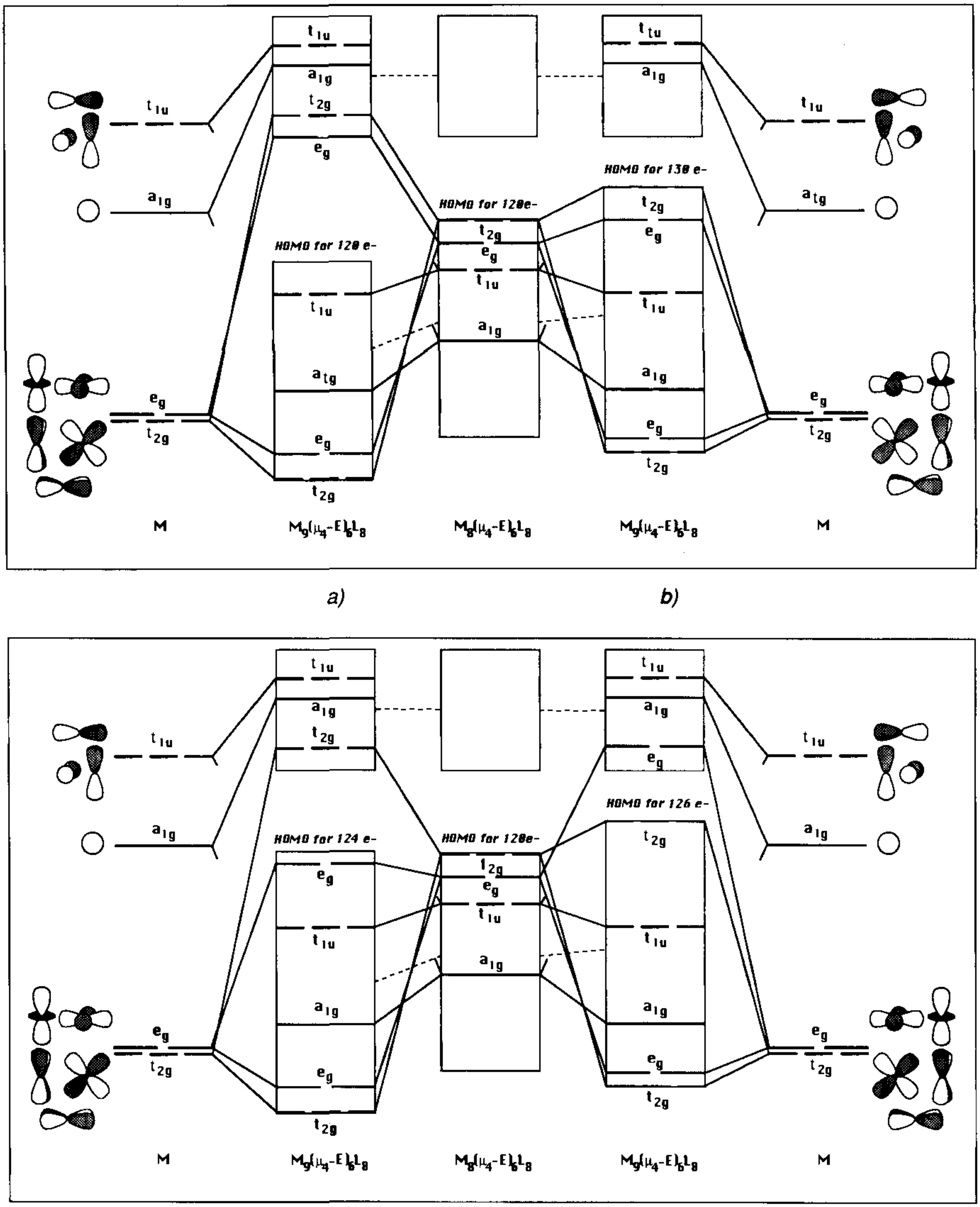

Figure 1. Qualitative MO diagrams (a–d) expected for a cluster $M_9(\mu_4\text{-E})_6L_8$ depending on the magnitude of the interaction of the central metal atom with its metallic host.

1, are given in Figures 2a and 3a, respectively. Both types of calculation are in good agreement (similar electronic configuration, energy gaps, and level ordering).

A large part of the bonding of the central Ni atom with its metallic host originates from strong interactions between the Ni_c vacant s and p orbitals with corresponding occupied metallic levels. The t_{2g} AOs of Ni_c point toward the Ni_s–Ni_s bonds and/or the Ni_s atoms. Strong interactions are then observed between this set of orbitals and d-type t_{2g} levels of the cage, particularly with the t_{2g} HOMO. This leads to a significant

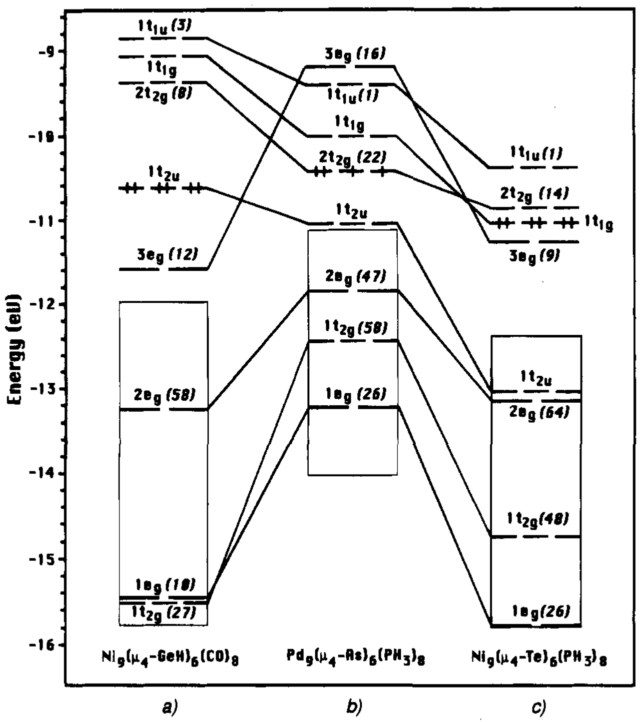

Figure 2. EH MO diagram for the models $Ni_9(\mu_4\text{-}GeH)_6(CO)_8$ (a), $Pd_9(\mu_4\text{-}As)_6(PH_3)_8$ (b), and $Ni_9(\mu_4\text{-}Te)_6(PH_3)_8$ (c). Numbers in parentheses indicate the percentage Ni_c character.

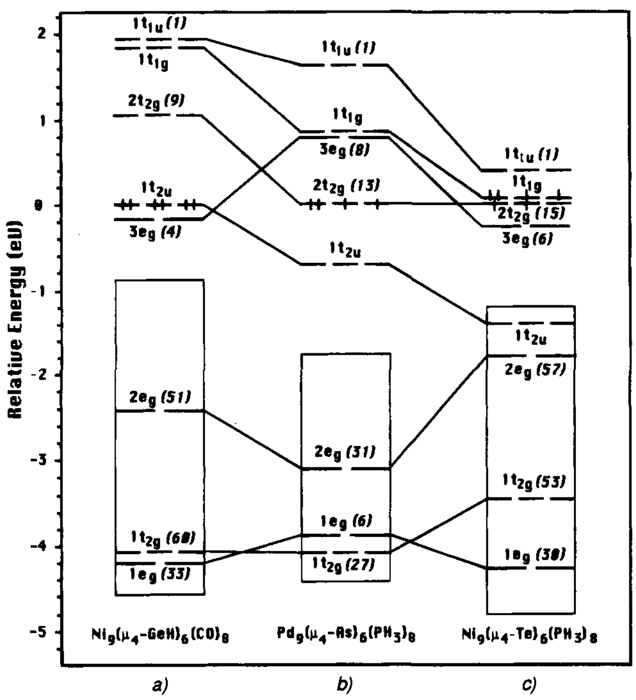

Figure 3. Xα MO diagram for the models $Ni_9(\mu_4\text{-}GeH)_6(CO)_8$ (a), $Pd_9(\mu_4\text{-}As)_6(PH_3)_8$ (b), and $Ni_9(\mu_4\text{-}Te)_6(PH_3)_8$ (c). Numbers in parentheses indicate the percentage Ni_c character. The zero energy has been arbitrarily set to the energy of the HOMOs.

stabilization of the in-phase combination ($1t_{2g}$) and a significant destabilization of the out-of-phase combination ($2t_{2g}$) which lies too high in energy to be populated. On the other hand, the situation is very different with the Ni_c e_g component. Indeed, they point toward the middle of the square faces of the cube where there is little Ni_s contribution. Therefore, the Ni_c e_g AOs interact poorly with the cubic framework, and the resultant Ni_c–Ni_s in-phase and out-of-phase combinations remain low in energy and can be occupied. This leads to an optimal total electron count of 124, corresponding to the electron configuration $[120](e_g)^4$, with a large HOMO ($1t_{2u}$)-LUMO ($2t_{2g}$) gap (1.2 and 1.1 eV with EH and Xα methods, respectively), in agreement with the color and diamagnetism of compound **1**.[2] Clearly, the MO diagram of $Ni_9(\mu_4\text{-}GeH)_6(CO)_8$ corresponds to the general situation depicted in Figure 1c. Note that a similar situation, but due to different orbital interactions, is encountered in the metal-centered early transition-metal halide octahedral clusters such as $Zr_6I_{12}(\mu_6\text{-}Fe)$, which possess four valence electrons more than the empty or main-group atom-centered analogs.[10]

Table 2. EH and Xα Electron Populations of the Valence Atomic Orbitals of the Central Metal Atom for the Given Ground-State Configurations in Different $M_9(\mu_4\text{-}E)_6L_8$ Models

compd		electron orbital population			
		s (a_{1g})	p (t_{1u})	d (e_g)	d (t_{2g})
$Ni_9(\mu_4\text{-}GeH)_6(CO)_8$	EH	0.66	0.49	3.98	5.10
$[120](e_g)^4$	Xα	0.46	0.43	3.83	5.02
$[Ni_9(\mu_4\text{-}Ge)_6(CO)_8]^{6-}$	EH	0.71	0.70	3.86	5.38
$[120](t_{2g})^4$	Xα	0.60	0.53	3.74	5.17
$pd_8(\mu_4\text{-}As)_6(PH_3)_8$	EH	0.29	0.20	3.21	5.50
$[120](t_{2g})^4$	Xα	0.69	1.15	3.63	5.59
$P_9(\mu_4\text{-}Sb)_6(PH_3)_8$	EH	0.28	0.20	3.35	5.59
$[120](t_{2g})^4$	Xα	0.70	1.09	3.69	5.61
$[Ni_9(\mu_4\text{-}PH)_6(PH_3)_8]^{10+}$ [120]	EH	0.38	0.39	2.97	4.59
$Ni_9(\mu_4\text{-}Te)_6(PH_3)_8$	EH	0.54	0.40	3.99	5.21
$[120](e_g)^4(t_{1g})^4(t_{2g})^2$	Xα	0.75	0.97	3.97	5.18

The calculated EH and Xα electronic populations on the central nickel atom, given in Table 2, reflect the electron transfer from the cage into the Ni_c 4s and 4p AOs (roughly one electron) and the rather strong t_{2g} interaction. Conversely, the e_g population is close to 4, indicating that these orbitals do not play any significant role in the Ni_c–Ni_s bonding.

Some EH bond overlap populations for $Ni_9(\mu_4\text{-}GeH)_6(CO)_8$ are represented with respect to energy in Figure 4. Neither the M–M nor the M–E bonding contacts are maximized for the count of 124 MVEs. The Ni_s–Ni_s overlap population is smaller than the Ni_c–Ni_s overlap population (0.090 vs 0.198), reflecting the ratio of 1.15 for the corresponding bond lengths. The Ni_s–Ge and Ni_c–Ge overlap populations are equal to 0.353 and 0.041, respectively. The latter indicates some weak-bonding interaction between the central atom and the capping Ge atoms. Note that in our model, the Ni_c–Ge contacts are only 17% longer than the Ni_s–Ge contacts.

An Alternative Open-Shell Configuration for the Count of 124 MVE: The Model $Pd_9(\mu_4\text{-}E)_6(PH_3)_8$ (E = As, Sb)

According to Table 1, the M_s–M_s distances do not vary only as a function of the MVE count. They seem also to change with the nature of the capping ligand E. For instance, with M = Ni, the M_s–M_s separation is *ca.* 0.15 Å larger in compounds **2**–**5** (which possess bare atoms as E ligands) than in **1** (which bears substituted capping units).[3-5] At first sight, a Ni_s–Ni_s distance larger in **1** than in **2**–**5** would be expected from the simple comparison of their MVE counts. In the case of M = Pd, one can note a difference of 0.15 Å for the Pd_s–Pd_s contacts in the 124-MVE compounds **6** and **7**, which differ only in the nature of E (As *vs* Sb).[3,6]

In order to understand the effect of the nature of E on the electronic structure of the clusters studied, we have undertaken

(10) (a) Hughbanks, T.; Rosenthal, G.; Corbett, J. D. *J. Am. Chem. Soc.* **1988**, *110*, 1511. (b) Johnston, R. L.; Mingos, D. M. P. *Inorg. Chem.* **1985**, *25*, 1661.

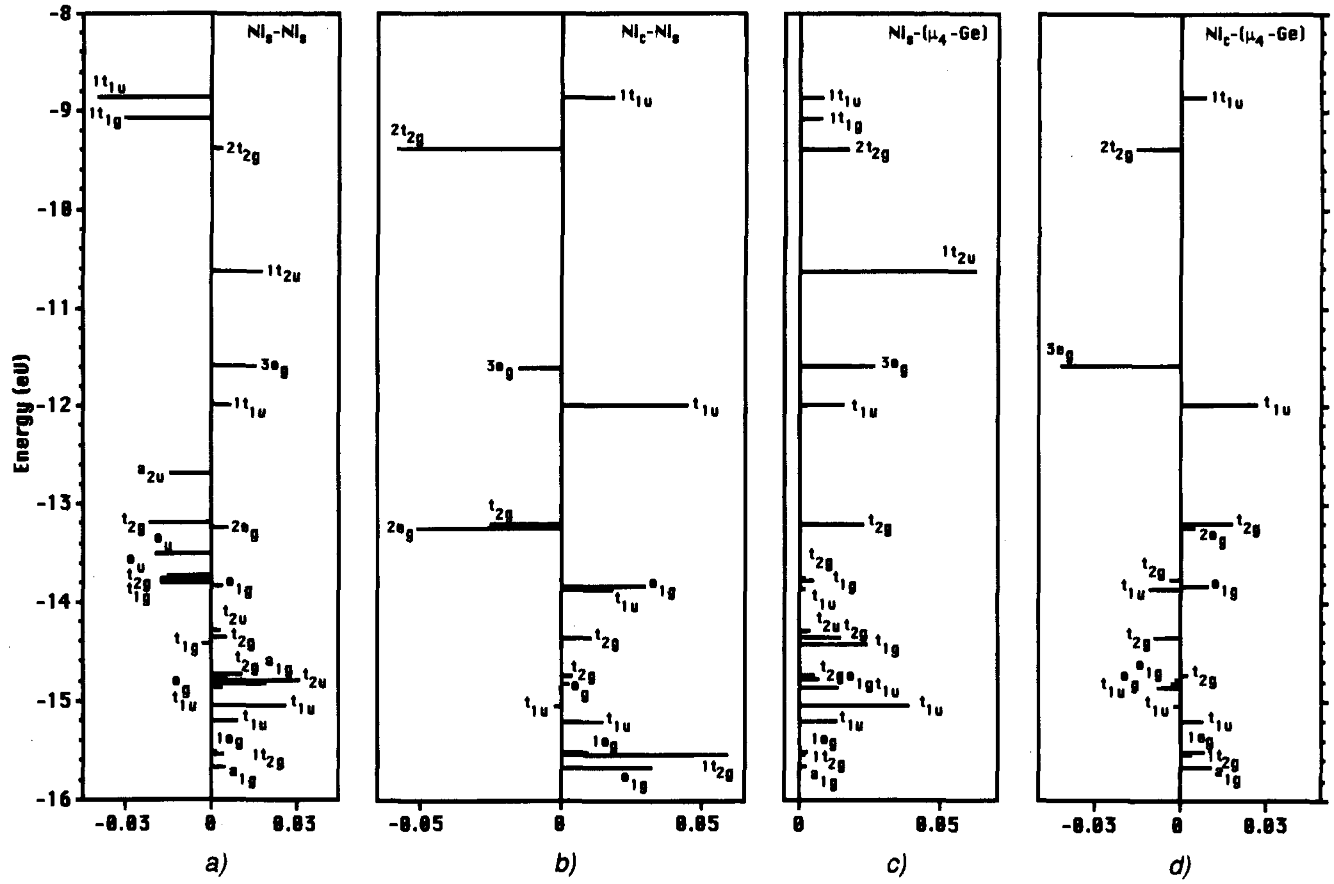

Figure 4. Ni_s-Ni_s (a), Ni_c-Ni_s (b), $Ni_s-(\mu_4\text{-Ge})$ (c), and $Ni_c-(\mu_4\text{-Ge})$ (d) overlap populations in $Ni_9(\mu_4\text{-GeH})_6(CO)_8$, obtained from EH calculations.

EH and Xα calculations on a 124-MVE cluster which possesses bare capping E ligands, namely $Pd_9(\mu_4\text{-As})_6(PH_3)_8$, used to model compound **6**. The EH and Xα MO diagrams, which are in rather good agreement, are shown in Figures 2b and 3b, respectively. Apart from the 5p shell, the calculated EH and Xα electronic populations on the central atom, given in Table 2, are also in reasonable agreement. Surprisingly, although both clusters $Ni_9(\mu_4\text{-GeH})_6(CO)_8$ and $Pd_9(\mu_4\text{-As})_6(PH_3)_8$ have the same 124-MVE count, their electron configuration differs. As stated above, the former adopts the closed-shell $[120](e_g)^4$ configuration, while an open-shell situation, $[120](t_{2g})^4$, is found for the latter.

A major question which arises then is the following: Why is there a $3e_g$-$2t_{2g}$ HOMO-LUMO level crossing when going from $Ni_9(\mu_4\text{-GeH})_6(CO)_8$ to $Pd_9(\mu_4\text{-As})_6(PH_3)_8$? The answer does not lie in the difference of magnitude of the e_g interaction between the capping E ligands and the central metal. This interaction is weak in the Pd, as well as in the Ni cluster, as illustrated by the e_g electronic population of the central Pd atom, close to 4, and comparable to that found for Ni_c in the Ni cluster. Since the reason appeared to originate from the difference in the electronic properties of a bare atom (such as As) and a conical fragment (such as GeR), we performed EH and Xα calculations on the model $[Ni_9(\mu_4\text{-Ge})_6(CO)_8]^{6-}$. This hypothetical 124-MVE species was generated from its parent $Ni_9(\mu_4\text{-GeH})_6(CO)_8$ model by simply removing the protons attached to the six Ge atoms, without any structural change, which allows an easy comparison between the two models. The same open-shell configuration as for $Pd_9(\mu_4\text{-As})_6(PH_3)_8$ is found, namely $[120](t_{2g})^4$. In fact, the Ni_c atom hardly perturbs the high-energy position of the out-of-phase $3e_g$ combination of $[Ni_9(\mu_4\text{-Ge})_6(CO)_8]^{6-}$. The destabilization of this level is still present when the central nickel atom is removed, as illustrated in Figure 5a, which shows the EH level ordering of the crucial metallic MOs of the non-centered $Ni_8(\mu_4\text{-Ge})_6(CO)_8$ and $Ni_8(\mu_4\text{-GeH})_6(CO)_8$ cubic cages. This is due to the energy difference of the σ-type frontier orbitals of Ge and GeR shown in Figure 5b. Because of the large energy gap between the 4s and 4p levels of Ge, the σ-type frontier orbital of a capping Ge atom can be identified as being a pure high-lying 4p AO. In the case of GeH, 4s/4p second-order mixing through the strong interaction with H leads to the formation of an sp hybrid of intermediate energy, much lower in energy than a pure 4p AO. When the six E ligands are assembled together to form an octahedral ligand shell, their σ-type frontier orbitals give rise to combinations of a_{1g}, e_g, and t_{1u} symmetry. These ligand combinations interact principally with metallic diffuse sp-type acceptor orbitals of the M_8L_8 cube.[1] However, they also have a destabilizing effect on some occupied d-type levels of the same symmetry. This effect is particularly favored with E = Ge, due to the high energy of its σ-type frontier orbital. The highest e_g level of the $Ni_8(CO)_8$ cage ($2e_g$ in Figure 5) is then pushed up above $3t_{2g}$ level. A similar situation occurs for the a_{1g} and t_{1u} levels, but, being lower in energy before interaction, their destabilizing effect is less effective, and no level of a_{1g} or t_{1u} symmetry goes above the $3t_{2g}$ level after interaction (see Figure 5).

Compared to that of $Ni_9(\mu_4\text{-GeH})_6(CO)_8$ (see above), the 4s and 4p populations of Ni_c indicate stronger a_{1g} and t_{1u} bonding interactions (mainly through $Ni_c\cdots Ge$ direct overlap) due to the higher energy of the a_{1g} and t_{1u} orbitals of the Ge_6 octahedron (see Table 2). This additional bonding partly counterbalances the destabilizing effect due to the partial occupation of the Ni_c-Ni_s antibonding $2t_{2g}$ HOMO. As a result, the EH Ni_c-Ge overlap population is larger in $[Ni_9(\mu_4\text{-Ge})_6(CO)_8]^{6-}$ (0.170 *vs* 0.041). The $3e_g$ MO is Ni_s-Ni_s bonding and slightly Ni_s-Ni_c antibonding, whereas the $2t_{2g}$ MO is strongly Ni_s-Ni_c anti-

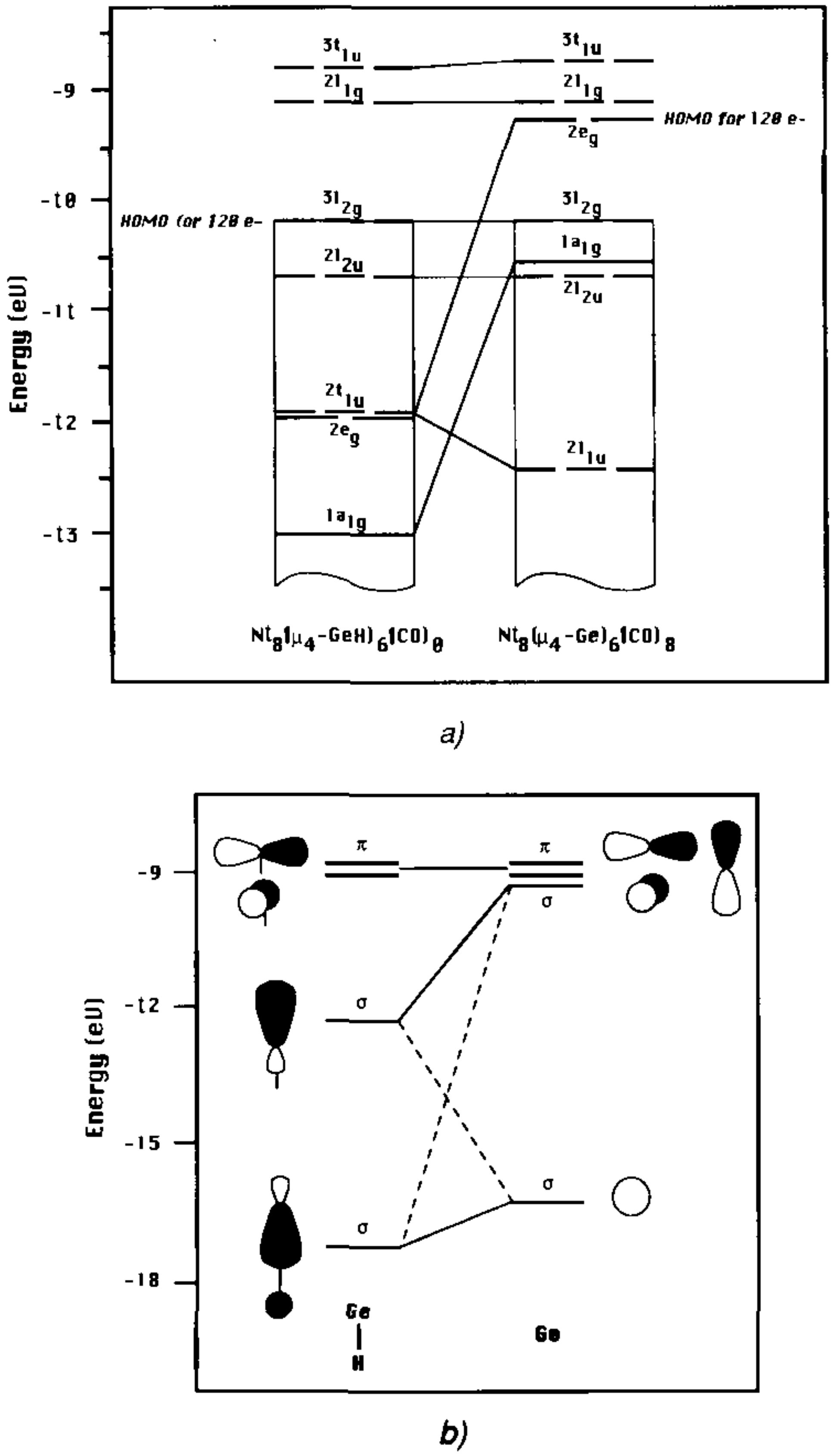

Figure 5. (a) Effect of the substitution of GeH by Ge on the EH MO diagram of the non-centered $Ni_8(\mu_4\text{-}Ge)_6(CO)_8$ and $Ni_8(\mu_4\text{-}GeH)_6(CO)_8$ cubic cage. (b) Comparison of the σ-type frontier orbitals of Ge and GeR (EH calculations).

bonding (see Figure 3). Therefore, when going from $Ni_9(\mu_4\text{-}GeH)_6(CO)_8$ to $[Ni_9(\mu_4\text{-}Ge)_6(CO)_8]^{6-}$, the depopulation of the $3e_g$ level to the benefit of the $2t_{2g}$ level should lead to a lengthening of the Ni−Ni separations, as suggested by the computed EH Ni_s−Ni_s and Ni_s−Ni_c overlap populations which are weaker in the latter (0.048 and 0.181, respectively). This is in agreement with the Ni−Ni distances measured in compounds listed in Table 1, which are longer in clusters having bare atoms as capping ligands.

The energy of the $3e_g$ level is crucial in deciding the ground-state configurations of the 124-MVE species. With substituted capping E ligands, the e_g component of the metallic $M_8(\mu_4\text{-}E)_6L_8$ host is always sufficiently low in energy to be occupied after interaction with the central metal atom, whatever its electronegativity. This leads to the $[120](e_g)^4$ closed-shell configuration. On the other hand, with bare atoms as capping ligands, the electronegativity becomes an important parameter. With electronegative E atoms, the $3e_g$ level is expected to remain at rather low energy, below the $2t_{2g}$ level, leading to the $[120](e_g)^4$ situation. With less electronegative atoms the $3e_g$ level is high in energy, leading to the $[120](t_{2g})^4$ situation. This is exemplified by EH calculations on the $[Ni_9(\mu_4\text{-}Ge)_6(CO)_8]^{6-}$ model where the atomic H_{ii} parameters of Ge were replaced by those of Te, anything else being kept the same. Under this condition, the ground-state configuration is $[120](e_g)^4$.

We have also carried out calculations on the 124-MVE cluster $Pd_9(\mu_4\text{-}Sb)_6(PH_3)_8$ used to model compound **7**. Although the Pd−Pd contacts are longer in this compound than in its As homolog **6** (see Table 1), our EH and Xα calculations indicate the same $[120](t_{2g})^4$ electron configuration, similar charge distribution (see Table 2), and level ordering for $Pd_9(\mu_4\text{-}As)_6(PH_3)_8$ and $Pd_9(\mu_4\text{-}Sb)_6(PH_3)_8$. We think that the electronegativity effect of the capping ligand is as important as the size effect in fixing the M_s−M_s bond lengths. If the electronegativity of the capping ligands is close to the electronegativity of the metal atoms (as in the case of **6**, Sb *vs* Ni),[11] strong covalence occurs between them, leading to a diminution of the metal

(11) (a) Pauling, L. *The Nature of the Chemical Bond*, 3rd ed.; Cornell University Press: Ithaca, NY, 1960. (b) Allred, A. L.; Rochow, E. G. *J. Inorg. Nucl. Chem.* **1958**, *5*, 264, 269.

character of the occupied MOs d block, and consequently to some weakening of their M_s-M_s antibonding character. This will favor short M_s-M_s separations. On the other hand, if the electronegativity difference is large (as in the case of **7**, As *vs* Ni),[11] the participation of the ligands into the metallic MOs is weaker, rendering them more strongly M_s-M_s antibonding. This will favor long M_s-M_s contacts.

Note Added in Proof. Analogous compounds, such as $Ni_9(\mu_4\text{-As})_6(P\text{-}n\text{-}Bu_3)_8$, $Ni_9(\mu_4\text{-Sb})_6(PPh_3)_8$, and $Ni_9(\mu_4\text{-Bi})_6(PPh_3)_8$, having the same electron configuation have been recently characterized (Vogt, K. Ph.D. Dissertation, University of Karlsruhe, Germany, 1994).

Electronic Structure of the Hypothetical 120-Electron Cubic Species $M_9(\mu_4\text{-E})_6L_8$

We mentioned above that, according to the electron-counting procedure of the inclusion principle,[7] the M_9 compounds should possess 120 MVEs, with the same electron configuration as the parent M_8 clusters. This electron count would be obtained if both of the out-of-phase t_{2g} and e_g combinations are strongly antibonding (see the Qualitative Approach section and Figure 1a). As mentioned in the preceding sections, the e_g AOs of M_c do not point toward the M_s atoms but toward the capping E ligands. This situation renders a strong e_g interaction difficult to realize. Indeed, the e_g frontier orbitals of the M_8 cage which are the closest in energy to the M_c e_g AOs are primarily d-type MOs, with a poor localization on E. Moreover, the M_c-E separation is rather large, always larger than the M_s-E separations (by 9−17% for the compounds listed in Table 1). A situation in which the E atom is small and/or the cube is large would force the capping ligands to approach the center of the faces of the cube and consequently would lead to shorter M_c-E distances, enhancing the e_g interaction. In addition, an increasing of the size of the M_8 cube leads to the destabilization of its $2e_g$ frontier orbital, which is M_s-M_s bonding.[1] As a consequence, the resulting antibonding $3e_g$ cluster MO is expected to lie at higher energy.

We have carried out EH calculations on the 120-MVE model $[Ni_9(\mu_4\text{-PH})_6(PH_3)_8]^{10+}$, which bears small E ligands. A variation of the Ni_s-Ni_s separation, keeping the Ni_c-P distances constant, shows a minimum energy for a Ni_s-Ni_s value of *ca.* 2.80 Å, *i.e.* for a large cube. As expected, the MO diagram of $Ni_9(\mu_4\text{-PH})_6(PH_3)_8$ is similar to that of $Ni_9(\mu_4\text{-GeH})_6(CO)_8$ depicted in Figures 2a and 3a, except that the $3e_g$ level now lies just above the $2t_{2g}$ orbitals. For the count of 120 MVEs, the computed HOMO ($1t_{2u}$)/LUMO ($2t_{2g}$) gap is vary large (1.9 eV). Clearly, this is the stable situation corresponding to the general case shown in Figure 1a, and illustrated by the rather weak 3d population of Ni_c (see Table 2). For this [120] configuration, the Ni_c-Ni_s and Ni_s-E (E = Ge or P) EH overlap populations are of the same order of magnitude in the two models, $[Ni_9(\mu_4\text{-PH})_6(PH_3)_8]^{10+}$ and $Ni_9(\mu_4\text{-GeH})_6(CO)_8$. On the other hand, the Ni_c-E overlap populations are very different (0.041 and 0.188 for Ge and P, respectively). Although we should be careful in comparing these values, we think that the latter reflects a significant bonding interaction. The Ni_s-Ni_s overlap populations are also significantly different (0.090 and 0.016 for the 124- and 120-MVE clusters, respectively). The 120-MVE count would correspond to an unrealistic charge of 10+ for species of formula $Ni_9(\mu_4\text{-PH})_6(PR_3)_8$. Therefore, a metal such as cobalt or rhodium seems more appropriate for attaining this low electron count, and compounds of the type $[M_9(\mu_4\text{-PR})_6(PR_3)_8]^+$ (M = d^9) can be suggested.[12] Another way to lower the positive charge of the Ni cluster model would be to encapsulate an early transition-metal atom at the center, though it appears chemically unlikely since the electronegativity of cluster centering atoms is rarely lower than that of the cage metals.[10a]

Electronic Structure of the 130-Electron Cubic Species $Ni_9(\mu_4\text{-Te})_6(PPh_3)_8$

A closed-shell configuration for 130 MVEs would be achieved if both the $3e_g$ and $2t_{2g}$ out-of-phase combinations were low in energy and occupied (see Figure 1b). Starting from the MO diagram corresponding to the closed-shell $[120](eg)^4$ ground-state configuration (see Figures 2a and 3a), one can realize that a strong stabilization of the $2t_{2g}$ level, which would be required for its occupation, could be obtained with a significant increase in size of the metallic cube. Indeed, long Ni_c-Ni_s separations are necessary to lower the antibonding character of this level. As a matter of fact, the 130-MVE compound **5** has particularly long Ni−Ni bonds (see Table 1).[5] EH calculations have been carried out on the model $Ni_9(\mu_4\text{-Te})_6(PH_3)_8$ of O_h symmetry. Assuming a closed-shell configuration, the actual electronic configuration shown in Figure 2c, $[120](e_g)^4(t_{1g})^6$, is somewhat different from that expected. Although bare Te atoms cap the metallic cube of $Ni_9(\mu_4\text{-Te})_6(PH_3)_8$, its electronic structure is closer to that of $Ni_9(\mu_4\text{-GeH})_6(CO)_8$ than to that of $Pd_9(\mu_4\text{-As})_6(PH_3)_8$.[8,9] Note that Te is more electronegative than As or Sb[11] (see above). The question which arises now is the following: Why are the six electrons expected to be in the $2t_{2g}$ level actually housed in the $1t_{1g}$ level? It turns out that the interaction between the t_{2g} orbitals of the M_8 and M_c fragments, although not strong, is still significant. The antibonding $2t_{2g}$ combination therefore lies at a rather high energy. On the other hand, the $1t_{1g}$ level, which has no Ni_c contribution by symmetry,[8,9] is strongly Ni_s-Ni_s antibonding at short separations.[1] This antibonding character is reduced for long Ni_s-Ni_s distances, as in **7**. The occupation of the Ni_s-Ni_s antibonding $1t_{1g}$ level renders the computed EH Ni_s-Ni_s overlap population particularly low (0.010). On the other hand, the Ni_c-Ni_s overlap population (0.156) is close to that found in $Ni_9(\mu_4\text{-GeH})_6(CO)_8$. The Ni_s-Te and Ni_c-Te overlap populations are 0.354 and 0.047, respectively.

Of course, the small HOMO/LUMO gap found in the EH calculations on $Ni_9(\mu_4\text{-Te})_6(PH_3)_8$ (0.25 eV) renders questionable the existence of a closed-shell ground state. In order to get more reliable information, Xα calculations have also been performed on the same 130-MVE model. The results, in terms of level ordering and charge distribution, are essentially similar (see Figure 3c and Table 2). All the $[120](e_g)^4(t_{1g})^{6-x}(t_{2g})^x$ (x = 0−6) configurations have been calculated. The $(t_{1g})^4(t_{2g})^2$ distribution is found to be the most stable, with the $1t_{1g}$ and $2t_{2g}$ levels almost degenerate. The $(t_{1g})^3(t_{2g})^3$ and $(t_{1g})^5(t_{2g})^1$ configurations lie less than 0.04 eV higher in energy. At the actual level of accuracy, it is not really possible to distinguish between these three configurations which one is the real ground state. The $(t_{1g})^6(t_{2g})^0$ and $(t_{1g})^0(t_{2g})^6$ configurations are less stable than the $(t_{1g})^4(t_{2g})^2$ configuration by 0.11 and 0.75 eV, respectively. This suggests that too many electrons in the $2t_{2g}$ level induce an important loss of bonding between the central and surface metal atoms, rendering the cluster unstable with respect to dissociation.

(12) Some particular molecular compounds containing a Co_9 core have been characterized: Whitmire, K. H.; Eveland, J. R. *J. Chem. Soc., Chem. Commun.* **1994**, 1335.

General Discussion

According to the calculations described above, we can conclude that, from the four closed-shell configurations proposed in Figure 1, the two involving a weak t_{2g} interaction, which correspond to the 126- and 130-MVE counts, are unlikely to exist. Indeed, it appears almost impossible to fully cancel this interaction, at least with metals from the groups IIIB and VIIIB. The orbital interaction requirements needed for the two other closed-shell configurations are easier to realize. The 124-MVE count, corresponding to Figure 1c, necessitates a weak e_g interaction and strong t_{2g} interaction. This situation occurs for rather short and rather long M–M and M_c–E distances, respectively. This is probably the easiest case to obtain with capping E ligands being either substituted conical fragments (such as in **1**) or sufficiently electronegative bare atoms. The 120-MVE count is favored if both e_g and t_{2g} interactions are strong. So far, this situation, depicted in Figure 1a, is hypothetical. It could be obtained with transition metals which are less electron-rich than Ni. Short M_c–E distances, *i.e.* a small size for E compared to that of M, should also favor such an electron count.

As said above, it appears impossible to fully cancel the antibonding character of the $2t_{2g}$ orbitals. Even when the M–M distances are rather long, as in $Pd_9(\mu_4\text{-}Sb)_6(PH_3)_8$, this level is still somewhat antibonding and lies in the middle of an energy gap. This situation favors its partial occupation. Therefore, at least two general cases can be drawn for $120 < \text{MVE} \leq 124$:

(a) When the capping ligand E is an electropositive bare atom, and/or when the M_c–E distances are sufficiently short, the $3e_g$ level is not accessible, and electron counts corresponding to a $[120](t_{2g})^n$ configuration are favored. This is the case for compounds **6** and **7** ($n = 4$) and also for compounds **2**–**4** ($n =$ 1 or 2). This is supported by our Xα calculations on the 120- to 124-MVE models $[Ni_9(\mu_4\text{-}P)_6(PH_3)_8]^{x+}$ ($x = 4-0$). All these models differ only by the occupation of the $3t_{2g}$ level, which lies 0.30 to 0.73 eV above the occupied $1t_{2u}$ level and 1.50 to 1.23 eV below the vacant and almost degenerate $1t_{1g}$ and $3e_g$ levels. This level ordering is similar to that calculated for $Pd_9(\mu_4\text{-}As)_6(PH_3)_8$ (see Figure 3b).

(b) When E is a substituted conical fragment or an electronegative bare atom, and when the M_c–E distances are long, the $3e_g$ level becomes accessible. Although none of the clusters reported in Table 1 corresponds to this case, electron counts corresponding to the $[120](e_g)^{n'}(t_{2g})^n$ ($n' = 4$ or even <4) configurations should be possible.

What is the largest number of electrons which can be accommodated in the antibonding $2t_{2g}$ orbitals, without rendering the cluster unstable? The 124-MVE compounds **6** and **7** have four electrons in their $2t_{2g}$ HOMO, while the 130-MVE species **5** has only two in these levels but four in the antibonding $1t_{1g}$ levels. As mentioned above, the large electron count of **5** causes long M–M distances, inducing the near degeneracy of the $2t_{2g}$ and $1t_{1g}$ levels. There are no examples of compounds reported with $124 < \text{MVE} < 130$. We can suggest, however, hypothetical species with the configurations $[120](e_g)^4(t_{2g},t_{1g})^n$, $[120](t_{2g},e_g,t_{1g})^n$, or $[120](t_{2g},t_{1g})^n$, depending on the accessibility of the crucial $3e_g$ level.

Related Compounds

Regular or distorted metal-centered M_9 cubic architectures have also been encountered in other species such as $Cu_{70}Se_{35}(PEt_3)_{22}$ (60 MVEs),[13] $[Co_9Bi_4(CO)_{16}]^{2-}$ (127 MVEs), $[Co_{14}Bi_8(CO)_{20}]^{2-}$ (192 MVEs),[12] and $Pd_9(\mu{:}\eta^5,\eta^2\text{-}As_2)_4(PPh_3)_8$ (130 MVEs).[3] The analysis of the bonding in some of these compounds is under progress in our laboratory.

It is also worth noting that Wheeler has theoretically examined the possibility of encapsulating main-group atoms at the center of the metallic cube.[8] EH calculations carried out on the model $Ni_8(\mu_8\text{-}Te)(\mu_4\text{-}Te)_6(H)_8$ led him to propose two favorable MVE counts, of 110 and 126, for these hypothetical species, in disagreement with the inclusion principle[7] which predicts 120 MVEs. From the results described above, the following possible electron counts and configurations for centered cubic clusters of the type $M_8(\mu_8\text{-}E')(\mu_4\text{-}E)_6L_8$ can be suggested:

(a) The capping E ligands are substituted conical fragments or sufficiently electronegative bare atoms. In this case, the electron configuration of the noncentered cage is [120]. Two cases are *a priori* possible. (i) The four valence s (a_{1g}) and p (t_{1u}) AOs of the central main-group E′ atom interact strongly, leading to a 120-MVE closed-shell configuration, namely [120]. (ii) Heavy main-group elements have their valence s AO lying very low in energy. Consequently, a weak a_{1g} interaction could occur in such a case, leading to a 122-MVE closed-shell configuration, $[120](a_{1g})^2$.

(b) The capping E ligands are electropositive bare atoms. In this case, the noncentered cage presents a rather high-lying $2e_g$ level. Starting from an electron distribution in the d-block of the case for which this e_g level is empty which we note [116] (*i.e.* [120] minus $(eg)^4$), two general situations are again *a priori* possible: (i) The a_{1g} interaction is strong, giving the possible closed shell configuration [116]. (ii) The a_{1g} interaction is weak, and the closed-shell distribution $[116](a_{1g})^2$ is favored. Note that in both cases open-shell configurations with the e_g level somewhat occupied, *i.e* $[116](eg)^n$ and $[116](a_{1g})^2(eg)^n$ ($n \leq 4$), can also occur.

None of these electron distributions fits with the closed-shell configurations predicted by Wheeler.[8] Interestingly, Fenske and collaborators have very recently characterized the structure of $Ni_8(\mu_8\text{-}As)(\mu_4\text{-}As)_6(PPh_3)_8$, which has 119 MVEs.[14] Note also that a Se atom has been encapsulated in the midle of a cube in $Cu_{20}(\mu_8\text{-}Se)Se_{12}(PEt_3)_{12}$.[13] Calculations on various $M_8(\mu_8\text{-}E')(\mu_4\text{-}E)_6L_8$ clusters are currently under way in our laboratory.[15]

Conclusion

From the calculations performed on metal-centered hexacapped $M_9(\mu_4\text{-}E)_6L_8$ clusters, it has been possible to understand why different MVE counts can occur for the same cubic molecular architecture. The preference for one MVE count over the others depends on several structural parameters, such as the M–M and M–E distances, as well as the nature, size, and electronegativity of the different elements constituting the cluster (M, E, and L). In all cases, however, there is a significant bonding interaction between the s and p AOs of the encapsulated atom and metallic orbital counterparts of the $M_9(\mu_4\text{-}E)_6L_8$ cage. The differences originate principally from the different way the e_g and t_{2g} d AOs of the central metal interact with the cubic cage, and from the nature of the capping ligand. Although open-shell configurations are the most common (compounds **2**–**7**), they never lead to strong Jahn–Teller distortions.[2–6] This is due to the high connectivity of the different atoms constituting the cluster. Making new bonds induces a lengthening or a breaking of other bonds. This situation is reminiscent of that encountered in solid-state chemistry, for body-centered-cubic metals for instance. Thus, it is interesting to mention that two situations coexist from the point of view of electron-counting

(13) Fenske, D.; Fleischer, S.; Fleischer, H.; Persau, C.; Oliver, C.; Vogt, K. *Z. Anorg. Allg. Chem.* In press.
(14) Fenske, D.; Krautscheid, H. *Angew. Chem., Int. Ed. Engl.* **1990**, *29*, 1452.
(15) Halet, J.-F.; Le Beuze, A.; Saillard, J.-Y. To be submitted for publication.

for these cubic species. The fisrt situation is that generally observed for stable molecular systems, *i.e.* closed-shell electron configurations corresponding to *magic* MVE counts (120 or 124) which result from a significant HOMO/LUMO gap. The second one is common in extended structures. It corresponds to a range of possible electron counts from 120 to 130, with no significant gap between the skeletal frontier orbitals and consequently with open-shell electron configurations generally preferred.

Acknowledgment. We are grateful to Dr. R. L. Johnston for helpful comments and Prof. D. Fenske, Dr. C. Oliver, and Dr. K. Vogt for providing results prior to publication.

Appendix

(a) Extended Hückel Calculations. Calculations have been carried out within the extended Hückel formalism[16] using the weighted H_{ij} formula.[17] The standard atomic parameters utilized were taken from the literature.[18] Unless specified in the text, the different models used were based on the idealized (O_h) experimental molecular compounds.[2,5,6] The following bond distances (Å) were used: Ni−Ni = 2.67, Ni−(μ_4-Ge) = 2.36, Ni−C(O) = 1.78, Ge−H = 1.60, and C−O = 1.14 in $Ni_9(\mu_4\text{-GeH})_6(CO)_8$; Ni−Ni = 2.80, Ni−($\mu_4$-P) = 2.21, Ni−P(H$_3$) = 2.25, and P−H = 1.42 in $Ni_9(\mu_4\text{-PH})_6(PH_3)_8$; Ni−Ni = 2.85, Ni−($\mu_4$-Te) = 2.55, Ni−P(H$_3$) = 2.25, and P−H = 1.42 in $Ni_9(\mu_4\text{-Te})_6(PH_3)_8$.

(b) SCF-MS-Xα Calculations. The standard version of the (spin-restricted) density functional SCF-MS-Xα method[19] was used and applied to models of O_h symmetry $Ni_9(\mu_4\text{-GeH})_6(CO)_8$, $[Ni_9(\mu_4\text{-Ge})_6(CO)_8]^{6-}$, $Ni_9(\mu_4\text{-Te})_6(PH_3)_8$, and $Pd_9(\mu_4\text{-E})_6(PH_3)_8$ (E = As, Sb). The considered molecular geometries were the same as those used for the EH calculations. The geometry used for the models $[Ni_9(\mu_4\text{-P})_6(PH_3)_8]^{x+}$ (x = 0−4) was based on that of compound **2**.[3] The atomic radii of the M_s muffin-tin spheres were chosen in order to be tangent along the edges of the cube. In order to have a better overlap with the M_s and E atoms, the M_c atomic radius was enlarged by 15%. The atomic radii of the muffin-tin spheres r (Å) and the exchange scaling parameters α were taken from the tabulation of Schwarz[20] for heavy elements and from a publication of Slater[21] for H. The maximum l values in the partial wave expansion included in the calculations were l = 2 for Ni, Pd, Ge, As, Te, and outer spheres, l = 1 for P, O, and C spheres, and l = 0 for the H sphere.

Supplementary Material Available: Tables of one-electron energies and charge distribution for $Ni_9(\mu_4\text{-GeH})_6(CO)_8$, $[Ni_9(\mu_4\text{-Ge})_6(CO)_8]^{6-}$, $Pd_9(\mu_4\text{-As})_6(PH_3)_8$, $Pd_9(\mu_4\text{-Sb})_6(PH_3)_8$, $Ni_9(\mu_4\text{-Te})_6(PH_3)_8$ and $[Ni_9(\mu_4\text{-P})_6(PH_3)_8]^{4+/2+}$ obtained from Xα calculations; tables of EH and SCF-MS-Xα parameters (9 pages). This material is contained in many libraries on microfiche, immediately follows this article in the microfilm version of the journal, can be ordered from the ACS, and can be downloaded from the Internet; see any current masthead page for ordering information and Internet access instructions.

JA940958S

(16) (a) Hoffmann, R. *J. Chem. Phys.* **1963**, *39*, 1397. (b) Hoffmann, R.; Lipscomb, W. N. *J. Chem. Phys.* **1962**, *36*, 2179.
(17) Ammeter, J. H.; Bürgi, H.-B.; Thibeault, J. C.; Hoffmann, R. *J. Am. Chem. Soc.* **1978**, *100*, 3686.
(18) (a) Tatsumi, K.; Hoffmann, R.; Yamamoto, A.; Stille, J. K. *Bull. Chem. Soc. Jpn.* **1981**, *54*, 1857. (b) Summerville, R. H.; Hoffmann, R. *J. Am. Chem. Soc.* **1976**, *98*, 7240. (c) Hoffman, D. M.; Hoffmann, R.; Fisel, C. R. *J. Am. Chem. Soc.* **1982**, *104*, 3858. (d) Hugbanks, T.; Hoffmann, R.; Whangbo, M.-H.; Stewart, K. R.; Eisenstein, O.; Canadell, E. *J. Am. Chem. Soc.* **1982**, *104*, 3876. (e) Whangbo, M.-H.; Gressier, P. *Inorg. Chem.* **1984**, *23*, 1228. (f) Thorn, D. L.; Hoffmann, R. *Inorg. Chem.* **1978**, *17*, 126. (g) Underwood, D. J.; Nowak, M.; Hoffmann, R. *J. Am. Chem. Soc.* **1984**, *106*, 2837.
(19) Johnson, K. H. *Adv. Quantum Chem.* **1973**, *7*, 143.
(20) (a) Schwarz, K. *Phys. Rev. B* **1972**, *5*, 2466. (b) Schwarz, K. *Theor. Chim. Acta* **1974**, *34*, 225.
(21) Slater, J. C. *Int. J. Quantum Chem.* **1973**, *7*, 533.